# Supporting Information for "Economically Efficient and Environmentally Sustainable Irrigation Potentials: a Spatially Explicit Global Assessment"

Felicitas D. Beier[1,2] *, Benjamin Leon Bodirsky[1], Jens Heinke[1], Kristine Karstens[1,2], Jan Philipp Dietrich[1], Christoph Müller[1], Fabian Stenzel[1], Patrick von Jeetze[1,2], Alexander Popp[1], Hermann Lotze-Campen[1,2]

[1]Potsdam Institute for Climate Impact Research (PIK)

[2]Humboldt-Universität zu Berlin (HU)

**Contents of this file**

1. Detailed Methods: LPJmL Model Description
2. Detailed Methods: Yield Value Gain Potential
3. Detailed Methods: Reserved Current Agricultural Uses

**Additional Supporting Information (Files uploaded separately)**

1. PIA_bycountry_a.xlsx
2. PIA_bycountry_b.xlsx
3. PIWC_bycountry_a.xlsx
4. PIWC_bycountry_b.xlsx

---

*Also funded by Deutsche Bundesstiftung Umwelt (DBU)

5. PIWW_bycountry_a.xlsx

6. PIWW_bycountry_b.xlsx

**Introduction**

This Supporting Information provides additional details to the methods applied in the article.

Additionally, country-level results of irrigation potentials (potentially irrigated areas (PIA); potential irrigation water consumption (PIWC); potential irrigation water withdrawals (PIWW)) for 235 countries are provided for two model setups as separate files: (a) under consideration of currently irrigated areas that affect the river flow; (b) not considering currently irrigated areas for irrigation potentials that are purely determined by economic considerations.

## 1. Detailed Methods: LPJmL Model Description

The Lund-Potsdam-Jena managed Land (LPJmL) model is a spatio-temporally explicit process-based model that simulates the growth and geographical distribution of 11 plant functional types (natural vegetation) and 12 crop functional types (field crops) and additionally pasture as well as (woody and herbaceous) bioenergy crops. It accounts for feedbacks between vegetation, the global terrestrial water, carbon, and nitrogen cycles, and energy fluxes (von Bloh et al., 2018; Schaphoff, von Bloh, et al., 2018; Lutz et al., 2019). The model simulates the terrestrial water balance considering precipitation, snow melt, seepage, interception, plant transpiration and soil evaporation resulting in daily simulations of runoff and discharge and considers its close interactions with plant vegetation in terms of plant growth and productivity that is linked to soil and atmospheric moisture (Schaphoff, Forkel, et al., 2018). It delivers consistent estimates for spatially explicit irrigated and rainfed potential crop yields, plant water uptake and surface runoff that are the basis for our model. Evaporation of irrigation water during the growing season is calculated based on the fraction of irrigation water in soil moisture and canopy interception (Rost et al., 2008).

The crop types considered in LPJmL are mapped to the crop types considered in our analysis using the following mapping (see table S1). Since LPJmL considers fewer crops than our analysis, LPJmL's groundnut is also the proxycrop for both oilpalm and cotton; maize is also the proxycrop for fodder (forage) and the 'other' crop category including fruits, vegetables and nuts; temperate roots represent both sugar beet and potatoes.

Irrigated and rainfed crop yields as well as consumptive blue water requirements are provided by LPJmL5 with unlimited nitrogen supply (von Bloh et al., 2018). As opposed to previous LPJmL versions (Sitch et al., 2003; Bondeau et al., 2007; Schaphoff, von Bloh, et al., 2018; Schaphoff, Forkel, et al., 2018), LPJmL5 includes an implementation of the global terrestrial nitrogen cycle and consistently accounts for water, grassland and crop management. Since the LPJmL4 and LPJmL5 model version have diverged during the Nitrogen cycle implementation phase, certain natural vegetation dynamics (Forkel et al., 2014) have not yet been included in the newest LPJmL5 version (von Bloh et al., 2018). For this reason, natural vegetation inputs, such as lake evaporation, runoff and monthly discharge are provided by its predecessor LPJmL4 (Schaphoff, von Bloh, et al., 2018; Schaphoff, Forkel, et al., 2018).

## 2. Detailed Methods: Yield Value Gain Potential

The difference of irrigated and rainfed crop yields as estimated by LPJmL provides the yield gain through irrigation in tons of dry matter. Negative yield gains (irrigated yield < rainfed yield) are technically possible because irrigation may lead to a shift in the growing period in LPJmL resulting in lower irrigated yields. In such cases, the irrigation yield gain is set to 0.

To account for country-specific management effects on yields (e.g. fertilizer and pesticide use; different crop varieties; mechanization; cropping intensity representing multiple cropping or fallow land), LPJmL potential yields are calibrated to meet country-level production as reported by FAO (FAO, 2021) using a multiplicative factor for both rainfed and irrigated yields. Note that both rainfed and irrigated yields are calibrated to FAO country-levels. A potential multiple cropping effect is therefore applied to both irrigated and rainfed yields and cannot capture the effect that irrigation may lead to an additional cropping season and increase yields by one or two additional harvests per year.

Figure S1 shows the potential yield value gain through irrigation in USD per hectare for the historical crop mix in 2010. It represents the areas that would achieve yield gains through irrigation considering irrigated and rainfed potential yields valued at global FAO average prices (in USD per tDM).

## 3. Reserved Current Agricultural Uses

To derive the grid cell area (in Mha) that was irrigated in the year 2010, we use the irrigated area share provided by the Land-Use Harmonization 2 (LUH2) data set presented in Hurtt et al. (2020) (Hurtt et al., 2019, 2020). LUH2 is based on the HYDE 3.2 data set (Klein Goldewijk et al., 2017) that estimates historically irrigated areas based on Siebert et al. (2015), Portmann, Siebert, and Döll (2010) and FAOSTAT data (FAO, 2021). To obtain grid cell specific crop area for the 19 crop types used in our analysis, we combine the spatially explicit LUH2 cropland map with national crop-type specific data from FAOSTAT that provides country-level harvested areas of crop items.

The LUH2 cropland map is subdivided into only five crop functional types (C3 annuals; C4 annuals; C3 perennials; C4 perennials; C3 nitrogen fixers). These five functional types are further disaggregated into crop groups using relative shares of area harvested on country level from FAOSTAT. Because rice plays a special role in terms of irrigation as well as greenhouse gas accounting, the spatial distribution of rice areas is especially important. We therefore determine the distribution of physical rice areas by assigning the country's rice production first to flooded areas provided at cellular level by LUH2. Upland (aerobic) rice is accounted by distributing country-level FAO rice areas beyond country-aggregated LUH2 flooded area (i.e. where FAO reports higher country-level rice areas than there are LUH2 flooded areas in the respective country) equally across the remaining country's cropland area. Note that flooded areas are not accounted as irrigated areas. For one, because flooded rice production is often only partially irrigated with blue water and often just retains the rainwater in paddies (Klein Goldewijk et al., 2017; Hurtt et al., 2020) and also because flooding fulfills a special management purpose in terms of pest control (Ampong-Nyarko & De Datta, 1991).

Given the area irrigated and the crop pattern in 2010 derived from LUH2 and FAOSTAT, the volume of current cellular irrigation water use ($U_{c,w}$) is calculated (see equation 1).

$$U_{c,w} = \sum_k V_{c,k,w} \cdot A_{c,k} \tag{1}$$

where $V_{c,k,w}$ refer to the crop water requirements per crop type ($k$) and grid cell ($c$) for the two water use types ($w =$ consumption and withdrawal), $A_{c,k}$ is the irrigated area per grid cell and crop.

## 4. Environmental Flow Requirements

The share of yearly discharge to be reserved for EFR per grid cell is calculated over a long-term reference period (1985-2015) based on monthly discharge provided by LPJmL4 (Schaphoff, von Bloh, et al., 2018). For a functioning freshwater ecosystem, a certain base flow (low flow requirements, LFR) is necessary to avoid aquatic species loss. Additionally, flooding plays an important role for riverine vegetation and wetlands. It can be accounted for by high flow requirements (HFR) (Smakhtin et al., 2004). We follow the Variable Monthly Flow (VMF) method introduced by Pastor, Ludwig, Biemans, Hoff, and Kabat (2014). It determines EFR using the flow variation throughout a year with different requirements for low-, intermediate- and high-flow months parametrized to a 'fair' ecosystem preservation status. In low-flow months (i.e. months in which mean monthly flow is smaller or equal to 40 % of the mean annual flow), 60 % of mean monthly flows are reserved for the environment; in intermediate-flow months (i.e. months in which mean monthly flow is greater than 40 %, but smaller than 80 % of the mean annual flow) 45 %; and in high-flow months (i.e. months in which mean monthly flow is greater than 80 % of the mean annual flow) 30 % of mean monthly flows is reserved (Pastor et al., 2014). We adopted this method by splitting EFR into LFR and HFR-equivalents. Discharge reserved in low-flow months is attributed to LFR, discharge reserved in high-flow months is attributed to HFR, and half of intermediate-flow requirements are attributed to LFRs and the other half to HFRs to appropriately consider the interaction of EFR and inaccessible discharge.

Not all water on Earth can easily be brought into productive use (Postel et al., 1996; de Fraiture et al., 2001). Especially highly variable flows are difficult to access for humans and could only be used for irrigation with appropriate storage infrastructure (reservoirs), which are costly to install. To account for such inaccessible (or hardly accessible) discharge, we use the coefficient of variation (CV) of monthly discharge over a reference period of 30 years (here: 1980-2010) assuming a functional relationship that leads to a decrease in accessibility with increasing long-term seasonal variability of discharge (see equation 2).

$$a_c = 2^{\frac{\sigma_c}{\mu_c}} \tag{2}$$

where $a_c$ is the share of discharge in cell $c$ that can be accessed, $\sigma$ is the standard deviation of long-term monthly discharge in cell $c$ and $\mu$ is the mean discharge of cell $c$ over the same long-term period. The CV is the ratio of the two ($\frac{\sigma_c}{\mu_c}$). With the monthly discharge time series provided by LPJmL4, the CV ranges between 0 and 19.11 resulting in a functional form as displayed in figure S2b). The bulk of the data lies between 0 and 3.61 with the 25$^{\text{th}}$ percentile at 1.08 and the 75$^{\text{th}}$ percentile at 2.09 (see figure S2a). Only a few grid cells show discharge variability that results in complete inaccessibility.

We assume that seasonally highly variable flows are difficult to access by humans, but may serve an ecosystem function similar to HFRs. The baseflow or LFR, on the other hand, cannot be served by such variable flows and must be left untouched by human intervention when the environmental flow protection is considered. For this reason, we split discharge reserved for EFR into HFRs and LFRs. When discharge is constrained based on the accessibility constraint, HFRs count towards the inaccessible discharge, while LFRs are excluded from human access in addition to inaccessible discharge.

**Natural Land Protection**

The following map shows areas of ecological importance following the Half-Earth protection approach based on the data provided by Kok et al. (2020). It includes currently protected areas based on the World Database of Protected Areas (WDPA), biodiversity hotspots (Mittermeier et al., 2005) and intact forest landscapes (Potapov et al., 2017). On top of these areas, at least 50 % of the land surface of each 'ecoregion' as described in Dinerstein et al. (2019) is protected.

**References**

Ampong-Nyarko, K., & De Datta, S. K. (1991). *A Handbook for Weed Control in Rice.* Manila, Philippines: International Rice Research Institute (IRRI).

Bondeau, A., Smith, P. C., Zaehle, S., Schaphoff, S., Lucht, W., Cramer, W., ... Smith, B. (2007, March). Modelling the role of agriculture for the 20th century global terrestrial carbon balance. *Global Change Biology*, *13*(3), 679–706. Retrieved 2020-10-04, from http://doi.wiley.com/10.1111/j.1365-2486.2006.01305.x doi: 10.1111/j.1365-2486.2006.01305.x

de Fraiture, C., Molden, D., Amarasinghe, U., & Makin, I. (2001, January). PODIUM: Projecting water supply and demand for food production in 2025. *Physics and Chemistry of the Earth, Part B: Hydrology, Oceans and Atmosphere*, *26*(11-12), 869–876. Retrieved 2021-01-07, from https://linkinghub.elsevier.com/retrieve/pii/S1464190901000995 doi: 10.1016/S1464-1909(01)00099-5

Dinerstein, E., Vynne, C., Sala, E., Joshi, A. R., Fernando, S., Lovejoy, T. E., ... Wikramanayake, E. (2019, April). A Global Deal For Nature: Guiding principles, milestones, and targets. *Science Advances*, *5*(4), eaaw2869. Retrieved 2021-12-10, from https://www.science.org/doi/10.1126/sciadv.aaw2869 doi: 10.1126/sciadv.aaw2869

FAO. (2021). *FAOSTAT Data* [Bulk Download]. Retrieved 2021-05-21, from http://www.fao.org/faostat/en/

Forkel, M., Carvalhais, N., Schaphoff, S., v. Bloh, W., Migliavacca, M., Thurner, M., & Thonicke, K. (2014, December). Identifying environmental controls on vegetation greenness phenology through model–data integration. *Biogeosciences*, *11*(23), 7025–7050. Retrieved 2021-09-27, from https://bg.copernicus.org/articles/11/7025/2014/ doi: 10.5194/bg-11-7025-2014

Hurtt, G. C., Chini, L., Sahajpal, R., Frolking, S., Bodirsky, B. L., Calvin, K., … Zhang, X. (2019). Harmonization of Global Land Use Change and Management for the Period 850-2015. *Earth System Grid Federation*. doi: https://doi.org/10.22033/ESGF/input4MIPs.10454

Hurtt, G. C., Chini, L., Sahajpal, R., Frolking, S., Bodirsky, B. L., Calvin, K., … Zhang, X. (2020, November). Harmonization of global land use change and management for the period 850–2100 (LUH2) for CMIP6. *Geoscientific Model Development*, *13*(11), 5425–5464. Retrieved 2021-09-24, from https://gmd.copernicus.org/articles/13/5425/2020/ doi: 10.5194/gmd-13-5425-2020

Klein Goldewijk, K., Beusen, A., Doelman, J., & Stehfest, E. (2017, December). Anthropogenic land use estimates for the Holocene – HYDE 3.2. *Earth System Science Data*, *9*(2), 927–953. Retrieved 2021-09-24, from https://essd.copernicus.org/articles/9/927/2017/ doi: 10.5194/essd-9-927-2017

Kok, M. T., Meijer, J. R., van Zeist, W.-J., Hilbers, J. P., Immovilli, M., Janse, J. H., … Alkemade, R. (2020, August). *Assessing ambitious nature conservation strategies within a 2 degree warmer and food-secure world* (preprint). Ecology. Retrieved 2021-11-30, from http://biorxiv.org/lookup/doi/10.1101/2020.08.04.236489 doi: 10.1101/2020.08.04.236489

Lutz, F., Herzfeld, T., Heinke, J., Rolinski, S., Schaphoff, S., von Bloh, W., … Müller, C. (2019, June). Simulating the effect of tillage practices with the global ecosystem model LPJmL (version 5.0-tillage). *Geoscientific Model Development*, *12*(6), 2419–2440. Retrieved 2021-11-12, from https://gmd.copernicus.org/articles/12/2419/2019/ doi: 10.5194/gmd-12-2419-2019

Mittermeier, R. A., Robles Gil, P., Michael, H., Pilgrim, J., Brooks, T., Goettsch Mittermeier, C., ... da Fonseca, G. A. B. (2005). *Hotspots Revisited: Earth's Biologically Richest and Most Endangered Terrestrial Ecoregions* (2nd ed., Vol. 12). Conservation International.

Pastor, A. V., Ludwig, F., Biemans, H., Hoff, H., & Kabat, P. (2014, December). Accounting for environmental flow requirements in global water assessments. *Hydrology and Earth System Sciences*, *18*(12), 5041–5059. Retrieved 2020-12-15, from https://hess.copernicus.org/articles/18/5041/2014/ doi: 10.5194/hess-18-5041-2014

Portmann, F. T., Siebert, S., & Döll, P. (2010, March). MIRCA2000-Global monthly irrigated and rainfed crop areas around the year 2000: A new high-resolution data set for agricultural and hydrological modeling: MONTHLY IRRIGATED AND RAINFED CROP AREAS. *Global Biogeochemical Cycles*, *24*(1), n/a–n/a. Retrieved 2021-09-25, from http://doi.wiley.com/10.1029/2008GB003435 doi: 10.1029/2008GB003435

Postel, S. L., Daily, G. C., & Ehrlich, P. R. (1996, February). Human Appropriation of Renewable Fresh Water. *Science*, *271*(5250), 785–788. Retrieved 2021-12-23, from https://www.science.org/doi/10.1126/science.271.5250.785 doi: 10.1126/science.271.5250.785

Potapov, P., Hansen, M. C., Laestadius, L., Turubanova, S., Yaroshenko, A., Thies, C., ... Esipova, E. (2017, January). The last frontiers of wilderness: Tracking loss of intact forest landscapes from 2000 to 2013. *Science Advances*, *3*(1), e1600821. Retrieved 2021-12-19, from https://www.science.org/doi/10.1126/sciadv.1600821 doi: 10.1126/sciadv.1600821

Rost, S., Gerten, D., Bondeau, A., Lucht, W., Rohwer, J., & Schaphoff, S. (2008, September). Agricultural green and blue water consumption and its influence on the global water system: GLOBAL WATER USE IN AGRICULTURE. *Water Resources Research*, *44*(9). Retrieved 2021-04-19, from http://doi.wiley.com/10.1029/2007WR006331 doi: 10.1029/2007WR006331

Schaphoff, S., Forkel, M., Müller, C., Knauer, J., von Bloh, W., Gerten, D., . . . Waha, K. (2018, April). LPJmL4 – a dynamic global vegetation model with managed land – Part 2: Model evaluation. *Geoscientific Model Development*, *11*(4), 1377–1403. Retrieved 2021-09-03, from https://gmd.copernicus.org/articles/11/1377/2018/ doi: 10.5194/gmd-11-1377-2018

Schaphoff, S., von Bloh, W., Rammig, A., Thonicke, K., Biemans, H., Forkel, M., . . . Waha, K. (2018, April). LPJmL4 – a dynamic global vegetation model with managed land – Part 1: Model description. *Geoscientific Model Development*, *11*(4), 1343–1375. Retrieved 2021-09-03, from https://gmd.copernicus.org/articles/11/1343/2018/ doi: 10.5194/gmd-11-1343-2018

Siebert, S., Kummu, M., Porkka, M., Döll, P., Ramankutty, N., & Scanlon, B. (2015). *Historical Irrigation Dataset (HID).* MyGeoHUB. Retrieved 2021-09-25, from https://mygeohub.org/publications/8/2 (Type: dataset) doi: 10.13019/M20599

Sitch, S., Smith, B., Prentice, I. C., Arneth, A., Bondeau, A., Cramer, W., . . . Venevsky, S. (2003, February). Evaluation of ecosystem dynamics, plant geography and terrestrial carbon cycling in the LPJ dynamic global vegetation model: LPJ DYNAMIC GLOBAL VEGETATION MODEL. *Global Change Biology*, *9*(2), 161–185. Retrieved 2021-09-27, from http://doi.wiley.com/10.1046/j.1365-2486.2003.00569.x doi: 10.1046/j.1365-2486.2003.00569.x

Smakhtin, V., Revenga, C., & Döll, P. (2004, September). A Pilot Global Assessment of Environmental Water Requirements and Scarcity. *Water International*, *29*(3), 307–317. Retrieved 2020-12-15, from http://www.tandfonline.com/doi/abs/10.1080/02508060408691785 doi: 10.1080/02508060408691785

von Bloh, W., Schaphoff, S., Müller, C., Rolinski, S., Waha, K., & Zaehle, S. (2018). Implementing the nitrogen cycle into the dynamic global vegetation, hydrology, and crop growth model LPJmL (version 5.0). *Geoscientific Model Development*, *11*(7), 2789–2812. Retrieved 2021-11-10, from https://gmd.copernicus.org/articles/11/2789/2018/ doi: 10.5194/gmd-11-2789-2018

| **Crop types considered in LPJmL** | **Crop types considered in this study** |
|---|---|
| Temperate cereals | Temperate cereals |
| Tropical cereals | Tropical cereals |
| Maize | Maize; Others (fruits, vegetable, nuts); Forage |
| Rice | Rice |
| Oil crops (soybean) | Soybean |
| Oil crops (rapeseed) | Other oil crops (including rapeseed) |
| Oil crops (groundnut) | Groundnuts; Oilpalms; Cotton |
| Oil crops (sunflower) | Sunflower |
| Pulses | Pulses |
| Temperate roots | Potatoes; Sugar beet |
| Tropical roots | Tropical roots (including cassava) |
| Sugar cane | Sugar cane |
| Biomass grass | Short rotation grasses |
| Biomass trees | Short rotation trees |

**Table S1.** Mapping of LPJmL crop types to crop types considered in our analysis.

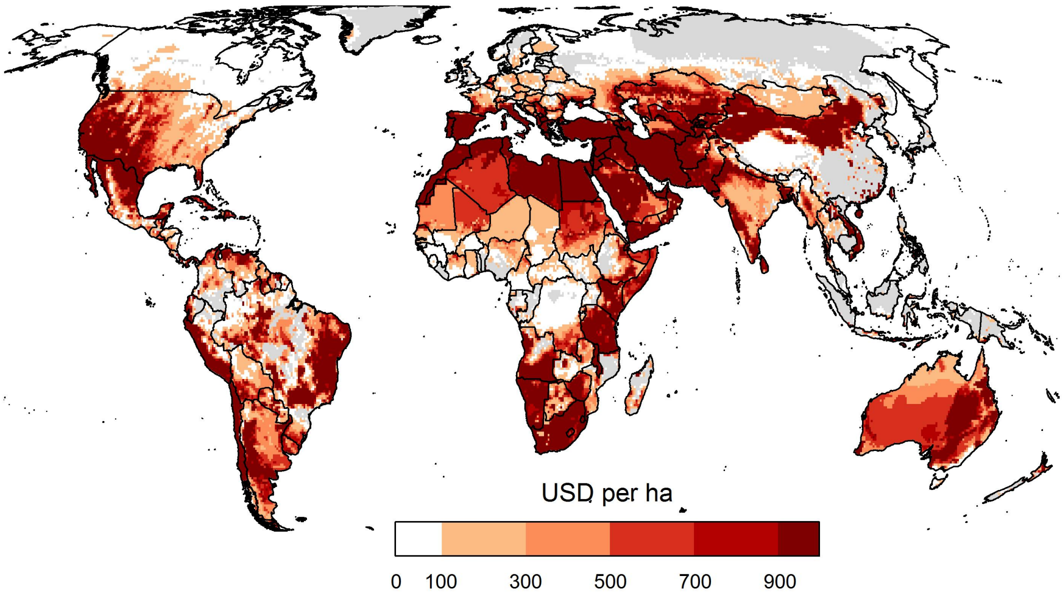


**Figure S1.** Potential yield value gain through irrigation in USD ha$^{-1}$. Areas in grey have a yield value gain of 0.

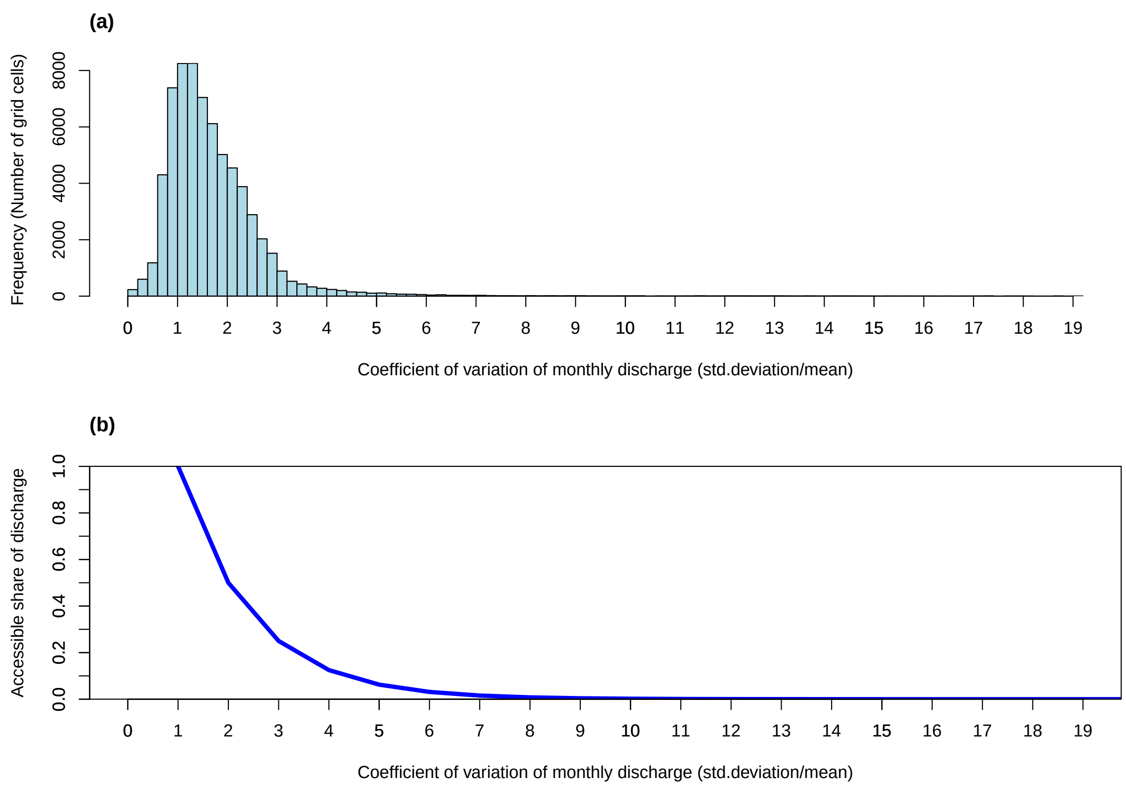


**Figure S2.** Frequency Coefficient of Variation of monthly discharge (a) and functional relationship between discharge accessibility share and coefficient of variation of discharge for time series of monthly discharge over the period from 1980 to 2010.

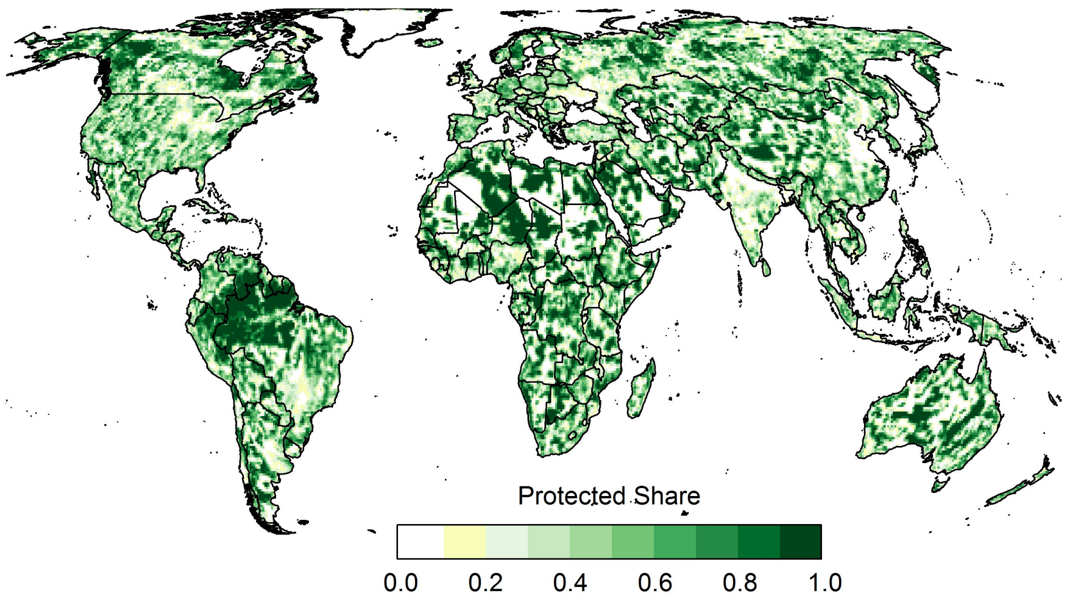


**Figure S3.** Share of grid cell that would be protected according to the Half-Earth protection approach.